Environmental Science Nano

Accepted Manuscript

ROYAL SOCIETY OF CHEMISTRY

rsc.li/es-nano

Impact of chemical composition of ecotoxicological test media on the stability and aggregation status of silver nanoparticles

George Metreveli[†], *Bianca Frombold*[†], *Frank Seitz*[‡], *Alexandra Grün*[§], *Allan Philippe*[†], *Ricki R. Rosenfeldt*[‡], *Mirco Bundschuh*[‡,#], *Ralf Schulz*[‡], *Werner Manz*[§], *and Gabriele E. Schaumann**[†]

[†]Group of Environmental and Soil Chemistry, Institute for Environmental Sciences, University of Koblenz-Landau, Fortstrasse 7, D-76829 Landau, Germany

[‡]Group of Ecotoxicology and Environment, Institute for Environmental Sciences, University of Koblenz-Landau, Fortstrasse 7, D-76829 Landau, Germany

[§]Department of Biology, Institute of Integrated Natural Sciences, University of Koblenz-Landau, Universitätsstrasse 1, D-56070 Koblenz, Germany

[#]Department of Aquatic Sciences and Assessment, Swedish University of Agricultural Sciences, Lennart Hjelms väg 9, SWE-75007 Uppsala, Sweden

Keywords: aggregation, attachment efficiency, critical coagulation concentration, humic acid, bridging

Abstract

Understanding of the interplay of generally known colloidal transformations under conditions of test media (TM) used during cultivation of organisms, biofilms and biological effect (=ecotoxicological) studies is still limited, although this knowledge is required for an adequate interpretation of test outcomes and for a comparison among different studies. In this context, we investigated aggregation and dissolution dynamics of citrate stabilized silver nanoparticles (Ag NP) by varying the composition of three TM (ASTM, SAM-5S, and R2A used during bioassays with *Daphnia magna*, *Gammarus fossarum*, and bacteria respectively) in the presence and absence of two types of natural organic matter (NOM), namely Suwanee River humic acid (SRHA) and seaweed extract (SW). Each original TM induced reaction-limited aggregation of Ag NP, and aggregation increased from R2A to SAM-5S and ASTM. In addition to the differences in aggregation dynamics, the concentration and speciation of Ag(I) differed between the three TM, whereby SAM-5S and ASTM are comparable with respect to the nature of the aggregation process, but clearly differ from the R2A medium. Furthermore, Cl^-, mainly present in SAM-5S, induced NP stabilization. The release of silver ions from Ag NP was controlled by the presence of NOM and organic constituents of TM, and by interactions with Cl^- and Br^-. The degree of aggregation, formation of interparticle cation-NOM bridges or stabilization was larger for Ca^{2+} than for Mg^{2+} due to the stronger ability of Ca^{2+} to interact with citrate or NOM compared to Mg^{2+}. These observations and the dependence of aggregation rates on the particle concentration renders interpretation of dose-response relationships challenging, but they may open perspectives for targeted ecotoxicological testing by modifications of TM composition.

Nano Impact

Ecotoxicological studies on engineered nanoparticles (NP) are conducted involving different test media (TM), whose composition is adapted towards the needs of the respective species. This composition significantly influences the colloidal state and properties of NP. In this work, aggregation and dissolution dynamics of Ag NP were characterized in three different TM by varying their composition. The dissolution of Ag NP was controlled by surface protection by natural organic matter (NOM) and organic constituents of TM, and by interactions with Cl^- and Br^-. In general, reaction-limited aggregation was observed. Aggregation depended predominantly on Ca^{2+}/Mg^{2+} ratio, anion composition and NOM quality. This knowledge will support the interpretation of and comparison among ecotoxicological studies that may have been performed under differing conditions.

Introduction

Assessing the potential environmental impact of engineered nanoparticles (NP) frequently involves the use of well-defined test media (TM), their composition has been carefully adapted towards the specific needs of the test organisms of interest. The different ionic and molecular backgrounds of the multitude of applied TM necessarily lead to a variety of NP transformations based on aggregation (in order to cover strongly as well as weakly bound NP clusters expected in TM, we use only the term “aggregation” regardless of the type of particle clusters), coating by TM constituents and interactions with organic matter (OM). Such transformations may affect the ecotoxicological potential of NP[1] and thus lead to TM-dependent biological responses. This may – at least partly – explain discrepancies of

ecotoxicological effect thresholds among studies. Despite this relevance, only limited information is available on potential NP transformations in TM up to now.

It is known that the typically high ionic strength in TM promotes aggregation of silver,[2-5] gold,[6] titanium dioxide,[1, 7-9] zinc oxide,[7, 10] and cerium dioxide[11] NP. Also, general impacts of individual TM constituents and additives (e.g., halides,[12-16] multivalent cations,[17-20] suspended minerals,[21] natural organic matter (NOM)[21, 22]) on NP transformations are well-known from lab studies in well-defined systems. Also, some studies specifically focused on the role of individual TM constituents or additives in complex systems: Nur et al.[9] observed that titanium dioxide NP aggregated according to the classical Derjaguin-Landau-Verwey-Overbeek (DLVO) theory despite the complex chemical composition of the test media. The critical coagulation concentration (CCC) of TM for titanium dioxide NP as determined by diluting the TM, varied between 18 and 54%,[9] which indicates that aggregation of these NP in the original (100%) TM is diffusion-limited. The dilution of TM in order to obtain stable Ag NP dispersions was also applied in other studies and suggested that dilution by a factor of 10, would reduce aggregation sufficiently for the tests.[2-4] Tejamaya et al.[4] reported increased shape and dissolution changes for citrate coated Ag NP after replacement of Cl^- by SO_4^{2-} and NO_3^-. Horst et al.[8] observed stabilizing effect of humic acid (HA) on titanium dioxide NP in TM. Besides these findings, it is still largely unknown, which of the generally known fundamental colloidal processes dominate NP transformation in which TM, to which extent the NP status varies among TM, and which aggregation mechanisms are relevant under which conditions. This knowledge is of high importance as the type of aggregation mechanism will influence among others, how strongly the NP status is governed by NP concentration and how the type of coating and the tendency for dissolution are expect to affect the ecotoxicological potential of NPs.

From systems containing a lower variety of constituents than most TM, it is known that besides the ionic strength, the type of cations and anions is important for the aggregation of NP. Divalent cations show higher efficiency to induce aggregation than monovalent cations.[17-20] Furthermore, aggregation of citrate coated Ag NP is more pronounced in the presence of Ca^{2+} compared to Mg^{2+}, which may be explained by the higher ability of Ca^{2+} to form complexes with citrate.[14, 18] Thus, not only differences in the total concentration of divalent cations, but also differences in the molar ratio of Ca^{2+} and Mg^{2+} in TM will result in different aggregation states and, thus, different ecotoxicological responses. Furthermore, TM composition differs with respect to presence and absence of halide ions. Chloride, for example, may either enhance or suppress the aggregation of Ag NP. An Ag NP stabilization by the formation of negatively charged AgCl(s) precipitates on NP surface was observed in several studies,[4, 12, 13] whereas Baalousha et al.[14] reported enhanced aggregation due to inter-particle bridging by solid phase AgCl(s).

Even more complex is the role of organic substances in the TM. Depending on the needs of the target organisms, TM contain various organic substances (proteins, enzymes, vitamins, glucose and other) at variable concentrations. Their role for the NP transformation in TM still requires investigation. Furthermore, NOM is increasingly used as NP-stabilizing additive to traditional TM.[1, 8] However, NOM can induce either stabilization or destabilization of NP, depending on the solution chemistry and the type of NOM used.[22] Especially, the interplay between bridging-determined aggregation, which is observed predominantly at high concentration of multivalent cations,[14, 18, 23-25] and electrosteric stabilization[23, 26, 27] will depend strongly on the quality of NOM and on the concentration as well as types of multivalent cations. As reported by Stankus et al.[24] Mg^{2+} induced the bridging-determined aggregation to a lower extent compared to Ca^{2+}. As TM normally contain a mixture of salts

and sometimes various NOM additives, it will be essential to understand the combined effects of NOM and all cations as well as their individual contributions to the transformation of NP. Special emphasis has to be put on differences between Mg^{2+} and Ca^{2+} and between NOM types and their ability to interact with these multivalent cations. Moreover, the suggested impeding impact of NOM on the Ag NP dissolution[28-30] seems to be highly relevant for ecotoxicological testing.[31] However, up to date, no study is available in which the TM composition was varied systematically in order to elucidate the underlying NP transformation mechanisms and identify dominating effects.

Furthermore, the concentration of NP influences their transformations in TM. For high NP concentrations (from 50 to 500 mg L^{-1}) as used in some ecotoxicological studies,[7, 8, 10, 11] aggregation is significantly accelerated.[32-34] Thus, dose-response relationships[7, 35, 36] may be further distorted by NP concentration-dependent dynamics in aggregation during the tests. Moreover, the concentration of NP available for the organisms can be changed by sedimentation of aggregated NP. This can additionally complicate the interpretation of ecotoxicological test results.[37]

On the example of silver nanoparticles (Ag NP), which are widely used in consumer products, the central aim of this study was to elucidate how and to which extent individual TM constituents trigger specific NP transformations and which mechanisms are responsible for these processes. In particular, we tested the following hypotheses: i) Aggregation of Ag NP in TM without NOM and other organic compounds is described by classical DLVO theory and it is predominantly determined by the concentration of Ca^{2+}. ii) The presence of halide ions or organic compounds in TM modifies the NP surface, but NP aggregation is still dominated by the concentration of Ca^{2+}. iii) Under the conditions of different TM, NOM generally suppresses aggregation via electrosteric stabilization and hinders Ag NP

dissolution. iv) NP size does not alter the aggregation mechanism, v) For NOM that interact strongly with Ca^{2+}, there is a threshold value of Ca^{2+} concentration above which electrosteric stabilization is overlaid by bridging-determined aggregation.

In order to evaluate these hypotheses, aggregation dynamics of citrate stabilized Ag NP was investigated in three TM: ASTM, SAM-5S, and R2A used during bioassays with *Daphnia magna*, *Gammarus fossarum*, and bacteria, respectively. In order to obtain process-based understanding, we characterized the influence of NOM, the cations Ca^{2+} and Mg^{2+}, the anions Cl^-, Br^-, SO_4^{2-}, and NO_3^- as well as the concentration of NP on the aggregation of Ag NP by systematic variation of the TM chemical composition. In order to understand the influence of the particle size on the NP transformations under TM conditions, we used NP in two different sizes (i.e., 30 nm and 100 nm). Furthermore, the release of silver from Ag NP was investigated in the presence, as well as in the absence of NOM.

Materials and methods

Deionized water (resistivity: 18.2 MΩ·cm, Direct-Q UV, Millipore) was used for sample preparation in all experiments.

Silver Nanoparticles

Ag NP (30 nm and 100 nm) were synthesized by a citrate reduction method modified from Turkevich et al.[38] (for details see SI). Hydrodynamic diameter of Ag NP was measured via dynamic light scattering (DLS) at a scattering angle of 165° and zeta potential was determined via electrophoretic light scattering technique and was calculated using the Smoluchowski equation[39] (both using Delsa Nano C, Beckman Coulter). In the aggregation experiments the zeta potential was measured 5 min after adding Ag NP to TM. Due to the

relatively low sensitivity of the electrophoretic light scattering at reduced particle number concentrations, which is expected in response to the aggregation over time, the zeta potential was not measured for longer exposure durations. Nanoparticles were additionally characterized by transmission electron microscopy (TEM; LEO 922 Omega, ZEISS) after nebulization of the suspensions using an ultrasonic generator onto a 3 mm copper grid covered with a combined holey and ultrathin (about 3 nm) carbon film (Ted Pella, Inc.).

Preparation of TM

ASTM medium (used during bioassays with *Daphnia magna*)[40, 41], SAM-5S medium (used during bioassays with *Gammarus fossarum*)[42], and R2A medium (used during cultivation of bacteria and conducting of biofilm bioassays) were prepared as outlined in Table S1, S2 and S3. ASTM contains vitamins, 0.107 mmol L^{-1} Cl^-, and in total 1.7 mmol L^{-1} Ca^{2+} plus Mg^{2+}, SAM-5S medium is free of organic compounds and contains 2.051 mmol L^{-1} Cl^-, 0.01 mmol L^{-1} Br^-, and 1.25 mmol L^{-1} Ca^{2+} plus Mg^{2+}, and R2A contains in total 0.2 mmol L^{-1} Mg^{2+}, various OM as well as Tween 80 (Table S4).

The TM were, if needed, amended with NOM as follows: Suwannee River HA (SRHA) standard II from the International Humic Substance Society (preparation method for SRHA stock solution see in supporting information SI) was used as model NOM. Additionally, seaweed extract (SW; Marinure®) from Glenside was used in experiments with ASTM due to its frequent use in ecotoxicological testing.[37, 43, 44] Total organic carbon (TOC) concentration was adjusted to 9.4 mg L^{-1} SRHA and 8.0 mg L^{-1} SW, respectively, corresponding to total mass concentration of 20 mg L^{-1} for both NOM. Whereas SRHA contains carboxylic and phenolic functional groups, SW contains polysaccharides with hydroxyl, carboxylic, and amino functional groups,[45] thus the two NOM are expected to have a different affinity to

multivalent cations. Following the categorization of NOM into NOM of aquatic origin and of rather terrestrial origin,[46] it may be postulated from their composition that SW is likely to resemble aquatic NOM, while SRHA rather resembles NOM of terrestrial origin, the latter due to its higher affinity to Ca^{2+}.[47]

In order to measure the concentration of metals in R2A medium, potentially originating from Na-Pyruvat, but also from other individual organic compounds, the solutions of each individual organic compound were prepared at same concentration as used in R2A medium. Metal concentration was measured in unfiltered and with 3 kDa membrane (Amicon Ultra-15 centrifugal filter device, Merck Millipore) filtered solutions by inductively coupled plasma optical emission spectrometer (ICP-OES, 720, Agilent Technologies).

Ag^+ Release

Due to higher specific surface and expected higher dissolution rate, Ag^+ release from Ag NP was investigated in batch experiments exemplary for 30 nm Ag NP in the absence and presence of the respective NOM. Ag NP stock dispersion, NOM stock solution and medium were introduced into 50 mL polypropylene centrifuge tubes (VWR). Concentration of Ag NP was set to 2 mg L^{-1}, which approximates the mean value of the broad concentration range used in ecotoxicological studies. All samples were prepared in triplicate. After shaking for 1 and 7 days using a laboratory shaker at 20 rpm (rotation angle: 180°, INTELLI-MIXER, NeoLab), two 8.5 mL aliquots from each sample were distributed in two ultracentrifuge tubes (polycarbonate) and centrifuged at 396000 *g* for 2 h (SORVALL WX 90 Ultra, Thermo Electron Corporation). This allows separation of Ag NP (cutoff: 2 nm) from the supernatant (SI), which contains Ag^+ and - if present - ultra-small Ag NP (<2 nm). This fraction is abbreviated as $Ag_{<2nm}$ in the following. After centrifugation, 5 mL supernatant was removed

from each tube. Supernatants from two aliquot samples were recombined in one 15 mL centrifuge tube (Polypropylene, VWR) to obtain a sufficient volume (10 mL) for the subsequent analysis. Ag concentration in the supernatant was finally determined by inductively coupled plasma mass spectrometer (ICP-MS, XSeries 2, Thermo Scientific) after acidification with 100 µL 65% HNO_3 (sub-boiled). The concentration of $Ag_{<2nm}$ in undiluted Ag NP stock dispersion was also determined.

Model calculations for Ag(I) species

In order to be able to compare our results with information about distribution of thermodynamically expected Ag(I) species in TM, the speciation calculation was done for $Ag_{<2nm}$ concentrations detected in Ag^+ release experiments with 1 d shaking duration using Visual MINTEQ software version 3.0.[48] The calculations were performed based on the assumption that the fraction $Ag_{<2nm}$ in ultracentrifuged samples solely represents dissolved Ag(I) species. Ag(I) speciation was calculated for a CO_2 equilibrium between air and aqueous phase. The input parameters used in the model calculations are presented in Table S9.

Long Term Aggregation

Long-term aggregation was investigated for 30 nm and 100 nm Ag NP in all TM in the absence and presence of the respective NOM. Therefore, Ag NP stock dispersion was added to the TM directly in the size measurement cuvette (total sample volume: 3 mL; Ag NP concentration 2 mg L^{-1}). The pH values are listed in Table S5 and were not significantly influenced by NOM and Ag NP. Samples were manually shaken for 2-3 s. Z-average hydrodynamic diameter was measured for first 60 min every 42 s as well as after 1 d and 7 d covering the typical duration of some toxicity tests, for example, those performed with *Gammarus fossarum*.[41, 49] As a control, particle size of Ag NP was measured in deionized

water at the same particle concentration over the same test duration. All experiments were performed in duplicates.

Early Stage Aggregation Kinetics

Early stage aggregation kinetics were investigated for 30 nm Ag NP (concentration 2 mg L^{-1}) in the absence and presence of NOM in all TM, but varying Ca^{2+} (as $CaSO_4$) or Mg^{2+} (as $MgSO_4$) concentration (0.1-12 mmol L^{-1}). For this, stock solutions of salts and organic compounds (Table S6, S7 and S8) were prepared. The previously calculated volume of deionized water and stock solutions was added directly into the size measurement cuvette. The samples prepared for Ca^{2+} and Mg^{2+} addition did not contain Mg^{2+} and Ca^{2+} ions respectively. Furthermore, ionic strength-dependent aggregation kinetics of Ag NP were investigated in mixtures of Ca^{2+} and Mg^{2+} at the Ca^{2+}/Mg^{2+} molar ratios 0.7/1 and 1/0.25 as used in ASTM and SAM-5S respectively. DLS measurements were conducted for the first 10 min every 30 s, starting 30 s after addition of Ag NP. Resulting pH values are shown in Table S5. All experiments were duplicated.

In order to elucidate the influence of vitamins on the aggregation of Ag NP in TM, early stage aggregation experiments were performed for 30 nm Ag NP in the absence and presence of $CaSO_4$ (0.7 mmol L^{-1}) in modified ASTM medium, which contained vitamins at different concentrations (B_1: 0.075, 0.5, 5 mg L^{-1}; B_7: 0.00075, 0.005, 0.05 mg L^{-1}; B_{12}: 0.001, 0.01, 0.1 mg L^{-1};). To exclude the influence of Mg^{2+} on the aggregation, the modified ASTM medium did not contain Mg^{2+} ions. To investigate the role of inorganic anions in the aggregation of Ag NP, early stage aggregation experiments were done for 30 nm Ag NP in deionized water and modified ASTM medium in the absence and presence of $CaSO_4$ (manufacturer and purity see in Table S1) $CaCl_2$ (manufacturer and purity see in Table S2),

$Ca(NO_3)_2$ ($Ca(NO_3)_2 \cdot 4H_2O$, ≥ 99%, p.a., Carl Roth), or $CaBr_2$ (99.5%, Alfa Aesar) at the same Ca^{2+} concentration (0.7 mmol L^{-1}). The modified ASTM medium did not contain Mg^{2+} ions and vitamins to exclude their influence on the aggregation. In order to test the influence of monovalent cations on the aggregation of Ag NP in R2A medium, early stage aggregation experiments were performed in deionized water at the same divalent cation concentration as detected in R2A medium (0.03 mmol L^{-1} Ca^{2+} as $Ca(NO_3)_2$, Table S12) and at different $NaNO_3$ (≥ 99%, p.a., Carl Roth) concentrations (0 - 60 mmol L^{-1}). In order to elucidate the role of individual organic constituents of R2A on the aggregation of Ag NP (30 nm), early stage aggregation experiments were done in Mg^{2+}-free R2A medium in the absence and presence of individual organic constituents and their mixtures at the same concentrations as present in medium. In addition, the influence of NP concentration on the aggregation pattern was investigated exemplarily in the NOM-free ASTM medium for particle concentration ranges of 0.1-10 mg L^{-1} (30 nm NP) and 1-10 mg L^{-1} (100 nm NP) as well as in Mg^{2+}-free R2A medium for particle concentration range of 0.5-10 mg L^{-1} (30 nm NP).

Evaluation of Aggregation Kinetics

The aggregation rate constant, *k,* is proportional to the initial change in the hydrodynamic diameter of the nanoparticles, D_{NP}, with time and inversely proportional to the initial particle concentration N_0 in the early aggregation stage:[17, 18]

$$k \propto \frac{1}{N_0}\left(\frac{\mathrm{d}\,D_{NP}(t)}{\mathrm{d}\,t}\right)_{t\to 0} \qquad (1)$$

$(\mathrm{d}D_{NP}(t)/\mathrm{d}t)_{t\to 0}$ was determined by linear regression[17, 18] for the first 180 s.

The attachment efficiency, α, was calculated by normalizing the aggregation rate constant of interest to the aggregation rate constant obtained for the diffusion limited aggregation regime (k_{fast}):[17, 18]

$$\alpha = \frac{1}{W} = \frac{k}{k_{fast}} = \frac{\frac{1}{N_0}\left(\frac{\mathrm{d}\,D_{NP}(t)}{\mathrm{d}\,t}\right)_{t\to 0}}{\frac{1}{(N_0)_{fast}}\left(\frac{\mathrm{d}\,D_{NP}(t)}{\mathrm{d}\,t}\right)_{t\to 0,\,fast}}, \qquad (2)$$

W is the stability ratio and k_{fast} is independent of the electrolyte concentration.[17, 18] The value of k_{fast} was obtained as a mean value of the aggregation rate constants at cation concentrations where no significant concentration dependency of aggregation rate constants was observed any more. Thus, for nanoparticles aggregating due to classical DLVO interactions[50, 51] (e.g., in the absence of NOM) α will increase from zero to one. $\alpha < 1$ indicates reaction-limited aggregation, while $\alpha = 1$ indicates diffusion-limitation. α in the presence of NOM was calculated by normalizing k in the presence of NOM to k_{fast} in the absence of NOM. $\alpha > 1$ indicates additional aggregation mechanisms (e.g., interparticle bridging).[25] The CCC was determined from the intersection of linear fitting functions of α under reaction and diffusion limited regimes in double-logarithmic scale.[25]

Results and discussion

Ag NP Characteristics

Ag NP were predominantly spherical; 20% (30 nm Ag NP) and 7% (100 nm Ag NP) was present as rods and triangles (Figure S1). DLS indicated a z-average hydrodynamic diameter of 31.2 ± 1.2 nm and 107.3 ± 1.9 nm and a polydispersity index of 0.37 ± 0.03 and 0.18 ± 0.03 (mean ± standard deviation, n = 3) for the 30 nm and 100 nm Ag NP, respectively. Since

the number weighting shifts much stronger the particle size distribution to the small particle sizes than volume weighting,[52] the volume weighted median particle diameter was calculated from TEM data in order to validate DLS results. The volume weighted median particle diameter obtained from TEM images under the assumption that all particles are spherical was 67 nm (30 nm Ag NP) and 95 nm (100 nm Ag NP). The differences of size obtained by DLS and TEM especially for 30 nm Ag NP is due to size and shape polydispersity which may have induced a systematic error in the determination of the average hydrodynamic diameter by DLS.[53, 54] Also the presence of non-spherically-shaped NPs as observed by TEM may have introduced some uncertainties during the data evaluation due to assumption of spherical shape for all particles. More detailed information on the particle size distribution of 30 nm Ag NP can be found in Metreveli et al..[23] The Ag NP revealed zeta potentials of -59.4 ± 1.6 mV and -58.9 ± 0.5 mV (mean ± standard deviation, n = 3) for 30 nm and 100 nm Ag NP, respectively. The highly negative zeta potential underlines the high stability (>1 year) of both Ag NP dispersions.

Ag^+ Release

In all experiments, the concentration of $Ag_{<2nm}$ was higher than the initial $Ag_{<2nm}$ concentration (1.1 ± 0.5 µg L^{-1}; Figure 1) and differed among the TM, which suggests significant and TM-dependent dissolution of Ag NP. In the absence of NOM, 5.2%, 0.5% and 0.1% of the initially spiked 2 mg L^{-1} total silver was released in ASTM, SAM-5S and R2A, respectively, resulting in $Ag_{<2nm}$ concentrations after one day from 3.9 ± 2.2 µg L^{-1} (R2A) to 105.6 ± 0.4 µg L^{-1} (ASTM). One possible explanation for the differences among TM might be their substantial difference in terms of Cl^- concentration (107 µmol L^{-1} in ASTM, 2051 µmol L^{-1} in SAM-5S and 0 µmol L^{-1} in R2A). Furthermore, SAM-5S contains Br^- (10 µmol L^{-1}), which is not present in ASTM and R2A medium and undergoes even stronger

312 interactions with Ag(I), such that an impact of Br^- even at this low concentration cannot be
313 excluded.

314 As reported in the literature, the dissolution and ecotoxicological impact of Ag NP is strongly
315 affected by the Cl^- concentration.[15, 16] Furthermore, the different conditions in the TM will
316 lead to TM-dependent Ag speciation and therefore to potentially different impacts on the Ag
317 NP status. Model calculations for equilibrium speciation of Ag(I) showed that for the $Ag_{<2nm}$
318 concentrations determined after one day in supernatant, the solution was undersaturated
319 regarding solid phase silver chloride AgCl(s) and silver bromide AgBr(s) (Table S10). While
320 in ASTM and R2A most of Ag was present as Ag^+, aqueous silver chloride AgCl(aq)
321 dominated in SAM-5S due to highest Cl^- concentration. The $Ag_{<2nm}$ concentrations measured
322 after one day in supernatant of ASTM (105.6 ± 0.4 µg L^{-1}) and SAM-5S (11.2 ± 0.5 µg L^{-1})
323 were close to saturation concentrations calculated for ASTM (169 µg L^{-1}) regarding AgCl(s)
324 and for SAM-5S (21 µg L^{-1}) regarding AgBr(s) (Table S11). This indicates that during
325 dissolution of Ag NP a part of released Ag^+ is likely transferred to AgCl(s) or AgBr(s)
326 leading to the lower dissolved Ag concentration in SAM-5S compared to ASTM due to the
327 lower solubility constant for AgBr(s).[55, 56] In addition, the formation of surface precipitates of
328 AgCl(s) and AgBr(s) as discussed below can hinder further dissolution of Ag NP.

329 The low release of silver in the R2A medium, in turn, is likely explainable due to proteins or
330 protein fragments present in the medium, which can form protein corona on the Ag-NP
331 surface[57, 58] and hamper the diffusion and adsorption of oxidants as observed for citrate
332 coated Ag NP in the presence of bovine serum albumin (BSA)[59] and luciferase.[57]
333 Furthermore, the removal of potentially formed Ag^+-protein complexes by centrifugation,
334 which cannot be fully excluded under the used centrifugation conditions, can result in
335 underestimation of Ag^+ release. Interestingly, after 7 d exposure time, the concentration of

$Ag_{<2nm}$ decreased in ASTM (24.9 ± 2.2 µg L^{-1}) and SAM-5S (7.1 ± 2.4 µg L^{-1}), but not in R2A. This effect may be explained by the interplay of several processes like dissolution of initial silver oxide layer, oxidation of Ag NP surface, precipitation of AgCl(s), and re-sorption of released Ag^+ onto NP surfaces. After complete dissolution of initial Ag_2O layer, the dissolution rate of Ag NP can be decreased since further dissolution is likely controlled by oxidation reaction of Ag NP surface.[16] The simultaneous formation of AgCl(s) precipitates can lead to decreasing concentration of $Ag_{<2nm}$ in the solution. Furthermore, the re-sorption of released Ag^+ onto NP surface cannot be excluded,[28, 60] which can be mediated by complexation sites provided by the free terminal carboxylate group of the citrate coating.[61] In contrast to ASTM and SAM-5S, no decrease in the concentration of $Ag_{<2nm}$ was observed in R2A after 7 d, which can be attributed to the absence of halide ions or to the above-mentioned protecting effect of sorbed proteins and their fragments.

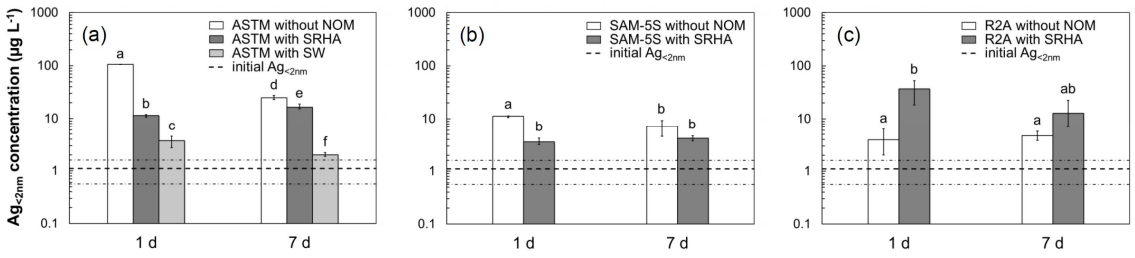

Figure 1. Release of $Ag_{<2nm}$ from 30 nm Ag NP (2 mg L^{-1}) in ASTM (a), SAM-5S (b), and R2A (c) medium with and without NOM for 1 d and 7 d exposure time. The error bars represent the minimal and maximal values of three replicates. The bold dashed lines correspond to mean initial concentration of $Ag_{<2nm}$ from three replicates. The fine dash-dot lines correspond to the minimal and maximal values of initial concentration of $Ag_{<2nm}$ from three replicates. Different letters denote statistically significant differences ($p < 0.05$, *t*-test). The data points with the same letters are not statistically different.

The presence of NOM decreased $Ag_{<2nm}$ concentration in ASTM and SAM-5S. The decrease in ASTM was stronger for SW than for SRHA. The observed effect of NOM agrees well with the previously reported decrease in Ag^+ release with increasing concentration of HA and

fulvic acid (FA).[28] This effect can be explained by physical protection of the Ag NP surface by adsorbed NOM[28, 29] or by reduction of Ag^+ by NOM[62, 63] and suggests a stronger protection by SW than SRHA. Stronger protection effect of SW may be explained by higher sorption of more hydrophilic[64] SW on hydrophilic Ag NP surface compared to SRHA. In contrast, SRHA increased the $Ag_{<2nm}$ concentration in the R2A TM, which either suggests a weaker protection by NOM in this medium or a meaningfully larger active Ag NP surface[60] than in the other media. The latter is supported by the smallest Ag NP sizes and complete stabilization found in R2A relative to ASTM and SAM-5S (Figure 2). Thus, dissolution of Ag NP in TM seems to be controlled by the interplay of protecting mechanisms reducing the reactivity of the Ag NP surface and stabilizing effects of NOM increasing the specific surface area of the Ag NP. The higher release of silver from Ag NP in all media by a factor of up to 2-100 compared to the original NP dispersions (Figure 1) underlines the relevance of this process during ecotoxicological tests, especially in the light of the substantial toxicity induced by Ag^+.[29] The interplay between protecting and dissolution-supporting effects of organic constituents of the TM as well as NOM additives needs, however, more attention to uncover the underlying chemical processes and mechanisms.

Long Term (≤7 d) Aggregation of Ag NP

In the absence of NOM, aggregation was observed in all TM, but not in deionized water (Figure 2 and Figure S2). Generally, aggregation rates of the 100 nm Ag NP were lower than those for 30 nm Ag NP. This difference may result from the lower initial particle number concentration and lower collision probability of 100 nm Ag NP compared to 30 nm Ag NP, but also differences in specific surfaces and thus NP reactivity towards aggregation cannot be excluded. This will be discussed on the basis of quantitative assessment of aggregation rates in the next chapter.

382 In the absence of NOM, Ag NP aggregation increased in the order: R2A < SAM-5S < ASTM
383 during the first day, whereas after seven days, Ag NP in SAM-5S showed a slightly higher
384 hydrodynamic diameter than in ASTM. Nonetheless, these differences should be interpreted
385 with care, since DLS analyses are biased in the presence of large aggregates. In ASTM and
386 SAM-5S, the hydrodynamic diameter of both Ag NP increased within the first day to 686-
387 1025 nm and 460-1089 nm, respectively. In R2A the 30 nm NP aggregated only within the
388 first minutes to 65 nm and then remained nearly constant, whereas the aggregation of 100 nm
389 Ag NP was much slower and aggregate size increased slightly up to 185 nm within one day
390 of exposure time (Figure 2e and 2f, Figure S2e and S2f). This effect can be explained again
391 by the lower initial particle number concentration and lower collision probability of 100 nm
392 Ag NP compared to 30 nm Ag NP.

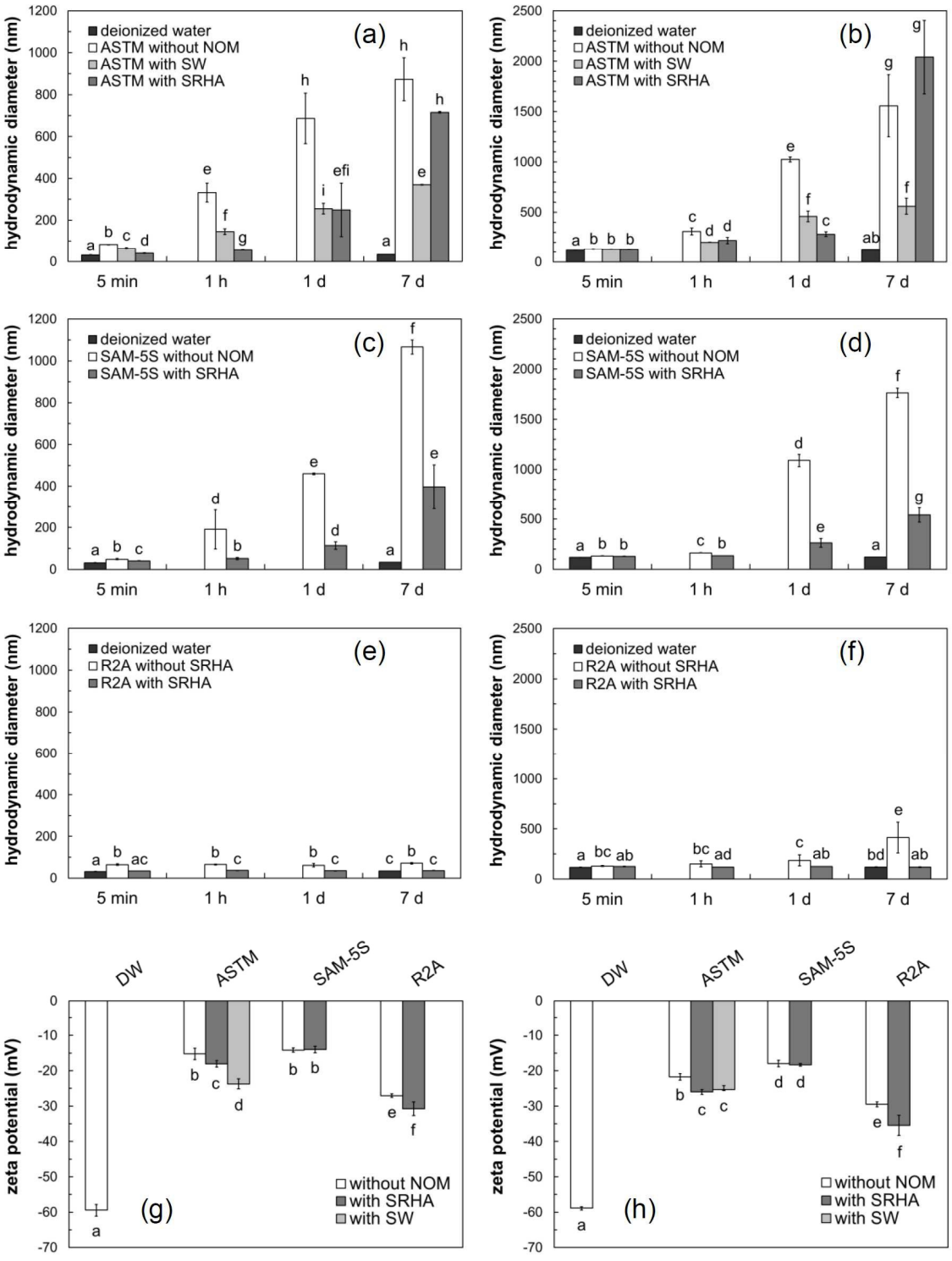

Figure 2. Mean hydrodynamic diameter of 30 nm (a), (c), (e) and 100 nm (b), (d), (f) Ag NP in ASTM (a), (b), SAM-5S (c), (d), and R2A (e), (f) medium as a function of exposure time and mean zeta potential of 30 nm (g) and 100 nm (h) Ag NP in deionized water (DW), ASTM, SAM-5S, and R2A medium in the absence, as well as

in the presence of NOM. Please consider the different y scales of Figures a, c, e with respect to b, d, f. Zeta potential was measured 5 min after adding Ag NP to TM. The error bars represent minimal and maximal values of two replicates. Different letters denote statistically significant differences ($p < 0.05$, *t*-test). The data points with the same letters are not statistically different.

Aggregation of Ag NP was consistent with the colloidal stability that can be expected from the zeta potential, which was most negative in the R2A medium although its absolute value was substantially reduced in all TM compared to deionized water (Figure 2g and 2h). The latter is a direct consequence of electrical double layer compression at high ionic strength (> 5mmol L^{-1}).[50, 51] Considering the respective ionic backgrounds in the different TM (Table S4) and the stability tendencies (Figure 2), it is clear that additional processes are involved in the stabilization of Ag NP. The medium R2A, which generated the most stable suspensions, contains among others the surfactant Tween-80. Tween-80 is known to readily adsorb onto the NP surface and stabilize NP[60] – a process potentially of high relevance for the present study. Furthermore, the stabilizing effect of the proteins[65] which are also present in the R2A medium, cannot be excluded.

NOM generally increased stability of Ag NP in all TM and at all points of time except for SRHA in ASTM in combination with 100 nm Ag NP after 7 days (Figure 2, Figure S2). These observations support the general expectation of electrosteric NP stabilization by NOM.[32-34] For exposure times exceeding one day SW served more efficiently as stabilizing agent relative to SRHA (Figure 2a and 2b), while for shorter exposure times, the stabilization by SRHA was slightly stronger or similar to SW. This could be explained by different adsorption kinetics of SRHA and SW to Ag NP or different aggregation mechanisms, which are further outlined below. However, neither SRHA nor SW completely prevented the Ag NP in ASTM and SAM-5S from aggregation as the hydrodynamic diameter continuously increased during the seven days (Figure 2c and 2d). In contrast to this, the addition of SRHA

to R2A even completely prevented aggregation after one minute (Figure 2e and 2f, Figure S2e and S2f) likely due to overlay of stabilizing effects of SRHA and surfactant Tween-80.

Another interesting finding is that the zeta potential became slightly more negative after addition of NOM in ASTM and R2A, but not in SAM-5S (Figure 2g and 2h). Although small, the differences range between 3-5 mV and are statistically significant. It can, thus, not be excluded that these differences reflect changes in NP surface charge. Thus, NOM alone was not able to modify the zeta potential in the presence of inorganic constituents (SAM-5S), but it may have been able to increase its absolute value in the presence of additional organic compounds (R2A and ASTM). Although the final explanation requires more detailed investigations, the results suggest an interplay between NOM and further organic compounds present in ASTM and R2A or solid phase AgCl(s) precipitates, which were most likely present on the surface of Ag NP in SAM-5S (see also discussion below).

If verified by further experiments, these findings demonstrate how the interplay between organic compounds and cations and its time dependence can affect dynamics in Ag NP stability. Therefore, using Ag NP pre-aged in TM likely results in different ecotoxicological effects relative to those used immediately after preparation, which was demonstrated for titanium dioxide NP in ASTM medium.[1]

Early Stage Aggregation Kinetics of Ag NP

The influence of particle number concentration on the initial aggregation rates of 30 nm and 100 nm Ag NP in ASTM is presented in Figure 3 on the basis of original aggregation data shown in Figure S3. The initial aggregation rates increased with increasing particle number concentration from 2.3 nm min^{-1} (100 nm Ag NP) to 38 nm min^{-1} (30 nm Ag NP), and within the limits of data scattering, this dependence can be described with one linear function,

suggesting comparable aggregation mechanisms for both particle sizes. Thus, no significant impacts of additional effects, such as specific surface or surface reactivity of the NP, are evident from our data. The lower initial aggregation rates of 100 nm NP compared to 30 nm NP can, thus, be explained by the lower particle number concentration and thus the lower collision probability. The linear relationship between initial aggregation rate and particle concentration is also in a good agreement with the classical DLVO theory. A similar linear increase of the initial aggregation rate with increasing particle number concentration was also observed for 30 nm Ag NP in Mg^{2+}-free R2A medium (Figure S4).

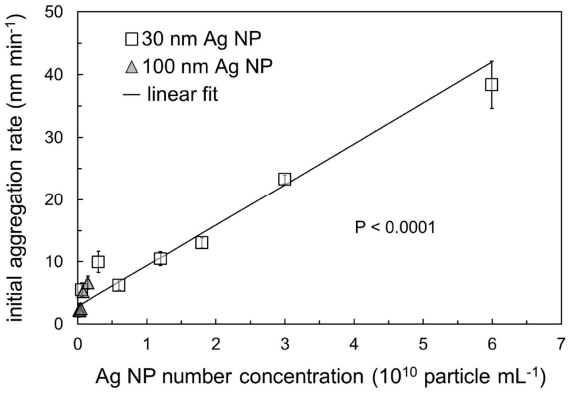

Figure 3. Mean initial aggregation rate of 30 nm and 100 nm Ag NP in ASTM medium as a function of particle number concentration. Mean values and standard deviations (error bars) were calculated from initial aggregation rates determined for the first 4, 5, and 6 min. Particle number concentration was calculated by the assumption that all particles are spherical and have the same particle diameter. Solid line represents the linear fit of combined experimental data for 30 nm and 100 nm Ag NP.

Attachment efficiency profiles obtained for the 30 nm Ag NP in the absence of NOM (Figure 4) showed two aggregation regimes (i.e., reaction and diffusion limited) and are in compliance with published literature.[17, 18] The CCC values ranged from 1.6 ± 0.1 mmol L^{-1} (Ca^{2+} in ASTM) to 2.3 ± 0.1 mmol L^{-1} (Mg^{2+} in SAM-5S) and were by a factor of up to 1.2 higher for Mg^{2+} than for Ca^{2+} and by a factor of 1.2-1.4 higher for SAM-5S than for ASTM (Table 1).

The slightly lower CCC and consequently, the higher efficiency of Ca^{2+} than Mg^{2+} to induce aggregation agrees well with the literature[14, 18] and can be explained by stability constants of citrate complexes formed on the surface of the citrate stabilized Ag NP, which are higher with calcium (logK = 8.02 for $CaHC_6H_5O_7$, logK = 3.5 for $CaC_6H_5O_7^-$) than with magnesium (log K = 7.66 for $MgHC_6H_5O_7$, logK = 3.38 for $MgC_6H_5O_7^-$).[66]

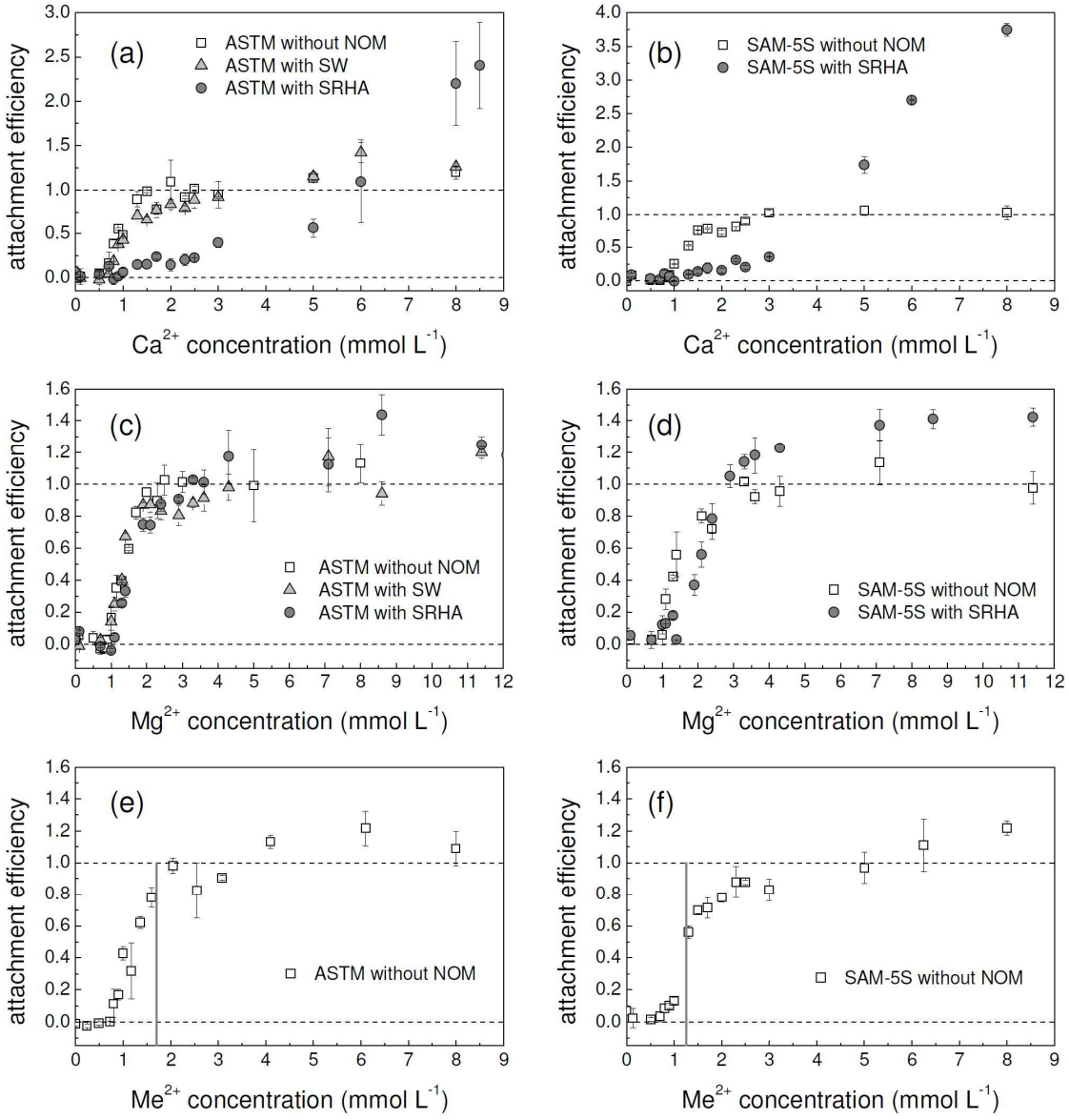

Figure 4. Mean attachment efficiency profiles of 30 nm Ag NP in cation-modified ASTM (a), (c), (e) and SAM-5S (b), (d), (f) medium in the absence, as well as in the presence of NOM for Ca^{2+} (a), (b), Mg^{2+} (c), (d), and for

mixture of both, Ca^{2+} and Mg^{2+} cations (e), (f). The samples prepared for Ca^{2+} and Mg^{2+} addition did not contain Mg^{2+} and Ca^{2+} respectively. Molar ratio of Ca^{2+} and Mg^{2+} was 0.7/1 for ASTM and 1/0.25 for SAM-5S medium. Me^{2+} concentration corresponds to the sum of Ca^{2+} and Mg^{2+} concentrations in the mixture. The grey vertical line shows the sum of Ca^{2+} and Mg^{2+} concentrations in the respective original medium. Horizontal dashed lines show the attachment efficiency values of 0 and 1. The values of $\alpha > 1$ indicate aggregation mechanisms not considered by the classical DLVO theory (e.g., interparticle bridging by cation-NOM complexes). The error bars represent the minimal and maximal values of two replicates.

On the other hand, the clearly higher CCC of Ca^{2+} and Mg^{2+} for SAM-5S than for ASTM despite comparable pH and divalent cation concentrations, indicate that in SAM-5S additional stabilization mechanisms are effective. Different concentrations of monovalent cations in the media cannot explain the differences in Ag NP stability since reported CCC of monovalent cations for citrate stabilized Ag NP (48-122 mmol L^{-1})[14, 18, 67] are much higher than their concentration in the medium (2.43 mmol L^{-1} in ASTM and 1.06 mmol L^{-1} in SAM-5S, Table S4). Therefore, other TM constituents, namely vitamins (present in ASTM) or halide ions (present in higher concentration in SAM-5S than in ASTM), are suspected to influence Ag NP stability.

Biotin (vitamin B_7), present in ASTM, for example, was found to form polymeric complexes through binding of Ag^+ to thioether and carbamide groups at concentrations of 2-25 mg L^{-1}.[55, 56] Although biotin concentration in ASTM is much lower than these values, it cannot be excluded that such polymeric complexes are also formed on the Ag NP surface and support particle aggregation in ASTM. In order to test this hypothesis, we measured the initial aggregation rates of 30 nm Ag NP in modified ASTM medium in the absence and presence of Ca^{2+} (0.7 mmol L^{-1}) as well as in the absence and presence of vitamins (B_1, B_7 and B_{12}) at different concentrations. The initial aggregation rate (ca. 2 nm min^{-1}) determined in the absence of vitamins did not change significantly in their presence even at 67 - 100 fold higher

vitamin concentrations than present in typical ASTM medium (Figure S5). This indicates that the vitamins used in ASTM medium do not influence the aggregation of Ag NP.

The concentration of Cl^- in SAM-5S medium is approximately 20 fold higher than in ASTM medium. Furthermore, SAM-5S medium contains Br^- ions, which are not present in ASTM medium. In order to evaluate the role of inorganic anions in the aggregation of Ag NP, we performed early stage aggregation experiments for 30 nm Ag NP in deionized water as well as in modified ASTM medium in the absence and presence of $CaSO_4$, $CaCl_2$, $Ca(NO_3)_2$, or $CaBr_2$ at the same Ca^{2+} concentration (0.7 mmol L^{-1}). In deionized water as well as in modified ASTM medium no aggregation occurred in the presence of Cl^- or Br^- (Figure 5a). In contrast to this, aggregation was observed in the presence of SO_4^{2-} or NO_3^- at the same Ca^{2+} concentration (Figure 5a). Our results are finally in a good agreement with El Badawy et al.[12], who reported much higher hydrodynamic diameter (determined by DLS) of Ag NP in the presence of 10 mmol L^{-1} $NaNO_3$ than in the presence of same amount of NaCl. In the solutions containing NaCl, no aggregation was observed even at low pH value (pH 3). El Badawy et al.[12] explained this effect by the high negative charge of AgCl(s) surface precipitates. The formation of solid phase AgCl(s) or AgBr(s) in our dispersions was confirmed by model calculations for the ASTM medium when modifying the anion composition by substitution of the $CaSO_4$ by $CaCl_2$ or $CaBr_2$ at equivalent Ca^{2+} concentration (0.7 mmol L^{-1}). The results of these calculations showed that 62.2% and 97.6% of the released silver was present as solid phase AgCl(s) and AgBr(s) respectively (Table S10). However, solid AgCl(s) precipitates or the presence of AgCl(s) colloids cannot easily explain a higher stability of Ag NP in the TM. On the other side, zeta potentials of Ag NP measured in ASTM medium modified with $CaCl_2$ or $CaBr_2$ were slightly more negative than in ASTM medium with $Ca(NO_3)_2$ (Figure 5b). Although these differences range only between 3 and 6

mV, they are statistically significant and they could support the idea that negatively charged surface precipitates of AgCl(s) or AgBr(s) may have stabilized nanoparticles in SAM-5S medium. Furthermore, the stabilization of nanoparticles by adsorption of Cl^- or Br^- cannot be excluded. The idea that halide ions stabilize the Ag NP in the TM is further supported by the observation that the CCC for citrate coated Ag NP determined by Li et al.[13] was higher for NaCl (40 mmol L^{-1}) than for $NaNO_3$ (30 mmol L^{-1}). Furthermore, Tejamaya et al.[4] reported a reduction of absorbance and appearance of a shoulder at higher wavelengths in surface plasmon resonance spectra for citrate coated Ag NP after substitution of Cl^- by SO_4^{2-} or NO_3^- in 10 fold diluted OECD test medium indicating similar to our results an increasing aggregation in the presence of SO_4^{2-} and NO_3^-. Partly opposite effects were reported in another study: Baalousha et al.[14] determined smaller CCC for citrate coated Ag NP in NaCl than in Na_2SO_4 and $NaNO_3$ electrolyte by UV-Vis measurements and explained this effect by increasing aggregation due to the possible bridging mechanisms by solid phase AgCl(s). In the presence of divalent cations (i.e., Ca^{2+} and Mg^{2+}) the influence of anions was less distinct, especially for the experiments using UV-Vis method for the detection of the CCC of Ca^{2+} and Mg^{2+}. The CCC determined by DLS was slightly higher for $CaCl_2$ than for $CaSO_4$ and $Ca(NO_3)_2$ which is in compliance with the above discussed results. Most likely, whether or not the presence of Cl^- or Br^- stabilizes the Ag NP depends on the concentrations of these anions and dissolution degree of Ag NP. In order to clarify to which extent the aggregation state of Ag NP depends on the concentrations of Cl^-, Br^-, and released Ag^+, further detailed investigations are needed.

Table 1. Mean CCC (in mmol L^{-1}) of 30 nm Ag NP in ASTM, SAM-5S, and R2A medium in the absence, as well as in the presence of NOM for Ca^{2+}, Mg^{2+} and for mixture of both, Ca^{2+} and Mg^{2+}.

	ASTM	SAM-5S	R2A

Ca^{2+} (without NOM)	1.6 ± 0.1	2.2 ± 0.1	n.d. [b]
Ca^{2+} (with SRHA)	6.3 ± 1.4 [a]	4.2 ± 0.1 [a]	n.d. [b]
Ca^{2+} (with SW)	3.5 ± 0.1	n.d. [b]	n.d. [b]
Mg^{2+} (without NOM)	1.9 ± 0.1	2.3 ± 0.1	1.7 ± 0.2
Mg^{2+} (with SRHA)	3.4 ± 0.1	2.9 ± 0.1	3.6 ± 0.1
Mg^{2+} (with SW)	2.0 ± 0.1	n.d. [b]	n.d. [b]
Ca^{2+} + Mg^{2+} (without NOM)	2.0 ± 0.1	2.4 ± 0.1	n.d. [b]

[a] This concentration does not represent classical CCC, but marks the cation concentration at which α becomes larger than 1, indicating the concentration range where non-classical DLVO interaction mechanisms like aggregation by bridging become more important. [b] n.d.: not determined.

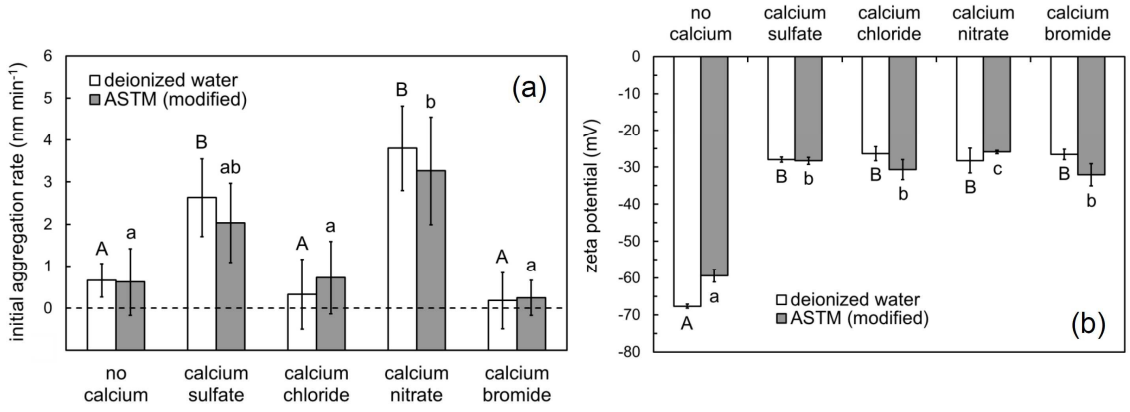

Figure 5. Mean initial aggregation rates (a) and mean zeta potentials (b) of 30 nm Ag NP in deionized water and modified ASTM medium in the absence and presence of $CaSO_4$, $CaCl_2$, $Ca(NO_3)_2$, or $CaBr_2$ at the same Ca^{2+} concentration (0.7 mmol L^{-1}). The modified ASTM medium did not contain Mg^{2+} and vitamins. The horizontal dashed line shows the initial aggregation rate when no aggregation occurs. The error bars represent the standard deviations from three replicates. Different letters denote statistically significant differences ($p < 0.05$, *t*-test) between the data points for deionized water (upper-case letters) and modified ASTM medium (lower-case letters). The data points with the same letters are not statistically different.

Despite the high long-term stability of Ag NP in R2A (Figure 2), which is most probably due to the presence of surfactants, it is important to mention that CCC of Mg^{2+} (1.7 ± 0.2 mmol L^{-1}) in R2A was even lower than in ASTM and SAM-5S in the absence of

559 NOM (Table 1), Furthermore, even in the absence of Mg^{2+}, attachment efficiency, α (0.15)
560 was clearly above zero (Figure 6), whereas aggregation of Ag NP in ASTM and SAM-5S
561 medium required Ca^{2+} or Mg^{2+} concentrations above 0.5-0.9 mmol L^{-1} (Figure 4). One reason
562 for these unexpected findings may be that the organic constituents of the R2A medium
563 contain significant amounts of cations, which had not yet been considered. The total
564 concentration of divalent (Ca^{2+} and Mg^{2+}) and monovalent (Na^{+} and K^{+}) cations originated
565 from the organic compounds of the R2A medium was 0.03 and 6.7 mmol L^{-1}, respectively
566 (Table S12). Considering that K^{+} (3.5 mmol L^{-1}) originated from K_2HPO_4, the total
567 monovalent cation concentration in Mg^{2+}-free R2A medium was approximately 10 mmol L^{-1}.
568 Additional experiments showed that aggregation of Ag NP in deionized water in the presence
569 of 0.03 mmol L^{-1} Ca^{2+} started at a Na^{+} concentration of approximately 30 mmol L^{-1} (Figure
570 S6). Therefore, monovalent and divalent cations available in Mg^{2+}-free R2A medium alone
571 cannot explain the increase in hydrodynamic diameter of Ag NP. Most likely, this effect is
572 induced by organic compounds present in R2A (amino acids, proteins and protein fragments;
573 Table S4) despite the high stabilization efficiency of Tween 80. Additional aggregation
574 experiments showed that in the absence of $MgSO_4$ the single organic constituents of R2A
575 medium alone did not induce aggregation of Ag NP (30 nm). Only the mixtures of individual
576 organic compounds were able to initialize aggregation (Figure S7). Most effective was the
577 mixture of casein and yeast extract, which contain amino acids, proteins and protein
578 fragments. Proteins adsorbing to Ag NP[57, 59, 68] can form a multilayer protein corona on NP
579 surfaces,[57, 58] which could also explain the fast initial increase in hydrodynamic diameter to
580 65 nm (Figure 2) instead of aggregation. However, additional aggregation experiments in
581 Mg^{2+}-free R2A at different Ag NP (30 nm) concentration showed that particle size remained
582 constant within 10 min, but it increased with increasing NP concentration (Figure S4), such
583 that even the initial increase in hydrodynamic diameter must be at least partly due to

aggregation, which is in contrast to the assumption of the sole relevance of the protein corona. Which mechanisms induce the initial aggregation and whether or not the protein corona is also effective (or becomes effective only slowly, preventing further aggregation after some minutes), should be investigated in further detail by assessing the development and architecture of OM coatings in media with complex composition.

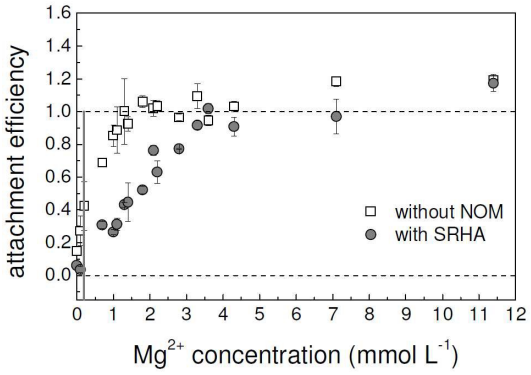

Figure 6. Mean attachment efficiency profiles of 30 nm Ag NP in cation modified R2A medium as a function of Mg^{2+} concentration. The grey vertical line shows the Mg^{2+} concentration in the original R2A medium. Horizontal dashed lines show the attachment efficiency values of 0 and 1. The error bars represent the minimal and maximal values of two replicates.

The attachment efficiency profiles for Me^{2+} used as Ca^{2+}-Mg^{2+} combinations at Ca^{2+}/Mg^{2+} ratio of the respective media (Figure 4e and 4f) indicated lower CCC of Me^{2+} in ASTM (2.0 ± 0.1 mmol L^{-1}) than in SAM-5S (2.4 ± 0.1 mmol L^{-1}). Thus, the media would have to be concentrated with respect to Me^{2+} concentration by a factor of only 1.2 for ASTM, but of 2.0 for SAM-5S in order to reach the diffusion limited regime.

This is in line with the findings for single cations. The total concentrations of divalent cations (Ca^{2+} + Mg^{2+} in ASTM and SAM-5S and Mg^{2+} in R2A) in all original TM (grey vertical lines in Figure 4e and 4f and Figure 6) lie in the reaction-limited regime, which predicts the formation of reaction-limited aggregates (RLA) in the original TM. It is important to note

603 that the Me^{2+} concentration in ASTM, but not in SAM-5S, is already close to the CCC, such
604 that an overlay between diffusion and reaction control cannot be excluded in ASTM. In
605 contrast to our observation for Ag NP, the results of Nur et al.[9] suggest diffusion limited
606 aggregation for titanium dioxide NP in several original TM. RLA are usually more compact
607 and stable compared to the diffusion-limited aggregates (DLA).[69] The difference in
608 aggregation regime between Ag NP and titanium dioxide NP, thus suggests that organisms
609 are confronted with different types of aggregates in the same test medium, depending on the
610 type of NP used.

611 Addition of NOM reduced α at the cation concentrations below respective CCC in all TM
612 (Figure 4) confirming the generally assumed stabilizing effect of NOM, which was stronger
613 in the presence of Ca^{2+} than in the presence of Mg^{2+} (Table 1). This is in contrast to the
614 strong destabilizing effect of Ca^{2+} on Ag NP in the absence of NOM. Moreover, the
615 stabilizing effect of SRHA in the presence of Ca^{2+} was dramatically stronger than that of SW,
616 and the differences between Ca^{2+} and Mg^{2+} in the presence of NOM were lower for SW than
617 for SRHA (Table 1 and Figure 4). This can be a result of stronger interaction between SRHA
618 and Ca^{2+} than between SRHA and Mg^{2+}, assuming that the multivalent cations act as bridging
619 agent between Ag NP and NOM coating. This is in line with the observation that in Ca^{2+}-
620 dominated systems, where the degree of SRHA-Me^{2+} interactions is higher compared to
621 Mg^{2+}-dominated systems.[24, 25]

622 In contrast to this, SRHA, but not SW, resulted in $\alpha > 1$ at Ca^{2+} concentrations above 6.3 ±
623 1.4 mmol L^{-1} for ASTM and above 4.2 ± 0.1 mmol L^{-1} for SAM-5S. Furthermore, α further
624 increased with increasing Ca^{2+} concentration up to 2.2 ± 0.5 and 3.7 ± 0.1 mmol L^{-1} in ASTM
625 and SAM-5S, respectively. Also high Mg^{2+} concentrations resulted in increased α (1.4), but
626 to a much lower extent than for Ca^{2+}. Such accelerated aggregation by SRHA in the presence

627 of Ca^{2+} in high concentrations is in line with observations for Ag NP[14, 18] and Au NP[24] in the
628 presence of FA or HA and has been explained by bridging of NP via Ca^{2+}-NOM complexes.
629 The formation of NP aggregates by cation-NOM bridges is not consistent with classical
630 DLVO theory. Stankus et al.[24] reported that Mg^{2+} can enhance NP aggregation in the
631 presence of SRHA (5 mg L^{-1} TOC), but to a lower extent than Ca^{2+}. The difference between
632 Ca^{2+} and Mg^{2+} was explained by the larger hydration radius of Mg^{2+} compared to Ca^{2+},
633 leading to a lower tendency of Mg^{2+} to form inner sphere complexes with the NOM.[24] The
634 fact that no effect was observed for Mg^{2+} in the work of Chen and Elimelech[25] is most likely
635 a result of significantly lower HA concentration (1 mg L^{-1} TOC) used in their work relative to
636 the present study (9.4 mg L^{-1} TOC). This demonstrates that, besides the concentration of
637 divalent cations, the NOM concentration is a key parameter influencing bridging-determined
638 aggregation.

639 The lack of aggregation enhancement by SW even in the presence of Ca^{2+} suggests that the
640 SW constituents tend to undergo insignificant bridging with Ca^{2+} and Mg^{2+}, which is most
641 probably due to differences in molecular weight, multi-functionality and affinity of functional
642 groups towards Ca^{2+} and Mg^{2+}. While SW contains large fraction of polysaccharides,
643 phenolic and carboxylic functional groups are relevant in SRHA, suggesting that coordinative
644 Me^{2+}-NOM interactions are more relevant in SRHA than in SW. In the presence of NOM
645 aggregation enhancement was also not observed in R2A medium, which underlines the
646 reported strong stabilizing efficiency of Tween 80.[60] Furthermore, other organic constituents
647 (proteins and protein fragments) of R2A may modified the Ag NP surface and by this
648 reduced the probability to form the Me^{2+}-NOM bridges between NP.

649 **Consequences for aggregation dynamics in test media**

Summarizing the findings of this study, TM-specific changes in Ag NP aging and aggregation state as well as in the concentration and speciation of Ag(I) are suggested (Table 2). Regarding the nature of the aggregation process, both SAM-5S and ASTM seem to be similar, but differ in the expression of qualitative characteristics of NOM coating and aggregate size. In contrast, the R2A results in clearly smaller aggregates and Ag^+ concentrations than the other two TM. Thus, although the characteristics of the Ag NP in R2A are not fully resolved, it seems unquestionable that they differ from those in the other two TM. Generally, under conditions of the investigated TM, the aggregation state of the Ag NP is determined by the Ca^{2+}/Mg^{2+} ratio and concentration of halide ions in the TM (Table 2).

In all TM, reaction-limited aggregates are expected, with the consequence that their morphology and stability is sensitive to the TM composition and NP concentration. These aggregates are very small in R2A medium, such that their properties will differ strongly from those of ASTM and SAM-5S. Aggregate types and dynamics are expected comparable between ASTM and SAM-5S medium, but zeta potential, aggregate sizes and NP reaction on the addition of different types of NOM and on the changes in concentration and composition of multivalent cations differs between these two media. Furthermore, the Me^{2+} concentration in ASTM is close to its CCC, suggesting starting relevance of diffusion-limitation for aggregation. These differences are mostly due to different initial molar ratios of Ca^{2+}/Mg^{2+} between the two media and the presence or absence of halide ions. In the absence of strong stabilizing agents like Tween 80, the most prominent differences among all TM are the concentration of Cl^- and the dominance of Ca^{2+}.

With respect to the inorganic constituents relevant for Ag NP dissolution, surface reaction and aggregation, the composition of the SAM-5S resembles that of the Rhine water discussed

674 by Metreveli et al.[23] and suggests that Ag NP aggregates are at least partly stabilized in the
675 presence of Cl^-, but with a distinct speciation of Ag(I) in this water. More generally speaking,
676 our results suggest that Ag NP may be only incompletely stabilized by NOM and halides in
677 natural waters, and NOM quality in addition to ion composition will strongly affect the nature
678 of the aggregates forming. Thus, as long as NOM in the natural water is similar to SW,
679 bridging-determined aggregates in that water will have low relevance compared to waters
680 rich in NOM similar to SRHA.

681 **Table 2.** Overview on NP characteristics in TM and their dynamics and changes upon modification of TM
682 composition as suggested from this study.

	ASTM	**SAM-5S**	**R2A**
Salt composition			
Ca^{2+}/Mg^{2+} [a]	0.69/1	1/0.25	0/0.2
Cl^-/Br^- [a]	0.11/0	2.05/0.01	0/0
Formation of Ag(I) species			
Ag^+ concentration	++++	++	+
predominant Ag(I) species	Ag^+	AgCl(aq)	Ag^+; Ag^+-protein complexes?
Impact of NOM	NOM reduces Ag^+ SW>SRHA	SRHA reduces Ag^+	SRHA increases Ag^+
Aggregation and colloidal stability			
Tendency to aggregate	++++	+++	+
$CCC(Mg^{2+})/CCC(Ca^{2+})$ [a]	1.9/1.6	2.3/2.2	1.7/n.d. [b]
NP stabilization	no effect of vitamins	by halide surface precipitates?	by Tween 80 protein corona?
Impact of NOM in original TM (at low Me^{2+} concentrations)	electrosteric stabilization SW ≤ SRHA (short term) SW > SRHA (long term)	electrosteric stabilization	electrosteric stabilization
Effect of Me^{2+} in the presence of NOM	Ca^{2+} enhances electrosteric stabilization compared to Mg^{2+} SRHA > SW		
	Me^{2+} induces bridging-determined aggregation at high concentrations:		no bridging-determined aggregation
	Ca^{2+}: > 6.3 mmol L^{-1}	Ca^{2+}: > 4.2 mmol L^{-1}	
	Mg^{2+}: > 3.4 mmol L^{-1}	Mg^{2+}: > 2.9 mmol L^{-1}	
General strength of cation effects	$Ca^{2+} > Mg^{2+}$ based on Me^{2+}-citrate and Me^{2+}-NOM interactions		

Expected characteristics relevant for ecotoxicological potential of Ag NP			
Dissolved species	++++ (Ag^+)	+++ (Ag^+; AgCl(aq))	+ (Ag^+)
NP surface	Ag-citrate	AgCl(s)	Ag-protein?
Effectiveness of NOM coating	+++	+++++	+
Aggregate size	++++	++++	+
Aggregate type	reaction-limited aggregates		reaction-limited aggregates small clusters?
	overlay with diffusion limitation		
Dynamic aggregation properties within test duration	aggregate size increases with time size and morphology strongly affected by NP concentration and solution chemistry		aggregate size constant, but depends on NP concentration
NOM-bridged aggregates	low relevance but expected relevance in hard water		

Impacts of changes in TM composition			
Addition of Cl^-	stabilizes NP, AgCl(s) on NP surface	enhances aggregation by AgCl(s)-bridging?	AgCl(s) on NP surface?
Reduction in Ca^{2+}/Mg^{2+} ratio	reduces aggregate size and stabilizing effect of SRHA coating		
Modifying NOM composition	SW: coating based on NOM-Ag interactions SRHA: coating based on Ca^{2+}-NOM interactions		effects overbalanced by Tween 80 effect?

[a] in mmol L^{-1} / mmol L^{-1}. [b] n.d.: not determined.

Conclusions

In summary, not only the composition of the TM but also the Ag NP concentration and the duration of the ecotoxicological and biological studies will significantly affect the aggregation status of Ag NP. This underlines the requirement to carefully interpret dose-response relationships and differences in toxicity towards the same organisms, which have been obtained for TM with different composition. In the absence of NOM, the formation of aggregates is controlled by the molar ratio of multivalent cations and by the type of anions. Under the conditions of TM, formation of bridging-determined aggregates induced by NOM is not relevant, but could increase in relevance in natural surface waters with high concentration of cations. Pre-aging of NP in the TM prior to the biological and ecotoxicological studies will minimize the time depending transformations and changes in

colloidal state and concentration of NP during the tests and will allow the investigation of the effect of different states of aggregation and different coating structures, but also of different concentrations of metal cations released from NP in the medium under conditions comparable with the realistic environmental scenarios.

The results of our study do not only show that by using different TM, the same Ag NP will likely have different ecotoxicological potentials, but they open perspectives for targeted research on the impact of individual Ag NP species on ecotoxicological potential. For example, increasing Ca^{2+}/Mg^{2+} concentration ratio in the absence of NOM will enhance aggregation. By modifying the nature of the NOM additive of the TM and the ratio between Ca^{2+} and Mg^{2+}, the effectiveness of the electrosteric stabilization by NOM will be modified and bridging-determined aggregation may be induced. The use of SW and the dominance of Mg^{2+} will favor aggregates formed on the basis of extended DLVO interactions. In ecotoxicological tests, these composition parameters could be adjusted within ranges where no or low effects on the vitality of test organisms are expected in order to obtain Ag NP with different coating stability, surface and aggregate characteristics, and concentration of dissolved Ag(I) species. It is furthermore essential to know how ecotoxicity results obtained in conventional TM could be transferred to environmental systems, the composition of which differs often significantly from that of the TM with the consequence of different aggregation properties.[6] Taking advantage of the knowledge of NP transformations in TM with modified chemical composition will, therefore, allow to predict specific NP characteristics and aggregation states in natural environmental systems, which may help in a second step to extrapolate ecotoxicological findings to the field.

Associated content

718 **Supporting information**

719 Details of the Ag NP synthesis method; Preparation method of SRHA stock Solution;
720 Calculation of centrifugation duration; Chemical composition of TM; pH values in TM after
721 addition of NOM and Ag NP; Chemical composition of the stock solutions used for early
722 stage aggregation experiments; Input parameters used in the model calculations; Speciation
723 of silver in TM; Metal concentrations in organic compounds used for preparation of R2A;
724 Particle size distribution (DLS) and TEM images of Ag NP; Hydrodynamic diameter of Ag
725 NP in TM for first 60 min as a function of exposure time. Hydrodynamic diameter of Ag NP
726 in ASTM and R2A at different particle concentrations; Initial aggregation rates of 30 nm Ag
727 NP in modified ASTM medium in the absence and presence of vitamins (B_1, B_7 and B_{12});
728 Initial aggregation rates of 30 nm Ag NP in deionized water in the presence of 0.03 mmol L^{-1}
729 Ca^{2+} and at different Na^{+} concentrations. Initial aggregation rates of 30 nm Ag NP in
730 deionized water and in Mg^{2+}-free R2A medium in the absence and presence of individual
731 organic constituents of R2A and their mixtures.

732 # Author information

733 **Corresponding authors**

734 *E-Mail: schaumann@uni-landau.de

735 **Notes**

736 The authors declare no competing financial interest.

737 # Acknowledgement

The authors thank the German Research Foundation (DFG) for financial support within research unit INTERNANO (FOR 1536 "Mobility, aging and functioning of engineered inorganic nanoparticles at the aquatic-terrestrial interface"); subprojects SCHA849/16; SCHU2271/5 and MA3273/3. We thank Bärbel Schmidt for her contribution to the aggregation and silver release experiments. We are also grateful to Dr. Wolfgang Fey for the ICP-MS measurements.

References

1. Seitz, F.; Luderwald, S.; Rosenfeldt, R. R.; Schulz, R.; Bundschuh, M., Aging of TiO_2 nanoparticles transiently increases their toxicity to the pelagic microcrustacean *Daphnia magna*. *Plos One* **2015,** *10*, (5).

2. Romer, I.; White, T. A.; Baalousha, M.; Chipman, K.; Viant, M. R.; Lead, J. R., Aggregation and dispersion of silver nanoparticles in exposure media for aquatic toxicity tests. *Journal of Chromatography A* **2011,** *1218*, (27), 4226-4233.

3. Romer, I.; Gavin, A. J.; White, T. A.; Merrifield, R. C.; Chipman, J. K.; Viant, M. R.; Lead, J. R., The critical importance of defined media conditions in *Daphnia magna* nanotoxicity studies. *Toxicology Letters* **2013,** *223*, (1), 103-108.

4. Tejamaya, M.; Romer, I.; Merrifield, R. C.; Lead, J. R., Stability of citrate, PVP, and PEG coated silver nanoparticles in ecotoxicology media. *Environmental Science and Technology* **2012,** *46*, (13), 7011-7017.

5. Zhao, C. M.; Wang, W. X., Size-dependent uptake of silver nanoparticles in *Daphnia magna*. *Environmental Science and Technology* **2012,** *46*, (20), 11345-11351.

6. Park, S.; Woodhall, J.; Ma, G. B.; Veinot, J. G. C.; Cresser, M. S.; Boxall, A. B. A., Regulatory ecotoxicity testing of engineered nanoparticles: Are the results relevant to the natural environment? *Nanotoxicology* **2014,** *8*, (5), 583-592.

7. Wiench, K.; Wohlleben, W.; Hisgen, V.; Radke, K.; Salinas, E.; Zok, S.; Landsiedel, R., Acute and chronic effects of nano- and non-nano-scale TiO_2 and ZnO particles on mobility and reproduction of the freshwater invertebrate *Daphnia magna*. *Chemosphere* **2009,** *76*, (10), 1356-1365.

8. Horst, A. M.; Ji, Z. X.; Holden, P. A., Nanoparticle dispersion in environmentally relevant culture media: A TiO_2 case study and considerations for a general approach. *Journal of Nanoparticle Research* **2012,** *14*, (8), 1014.

9. Nur, Y.; Lead, J. R.; Baalousha, M., Evaluation of charge and agglomeration behavior of TiO_2 nanoparticles in ecotoxicological media. *Science of The Total Environment* **2015,** *535*, (Special Issue: Engineered nanoparticles in soils and waters), 45-53.

10. Vielkind, M.; Kampen, I.; Kwade, A., Zinc oxide nanoparticles in bacterial growth medium: Optimized dispersion and growth inhibition of *Pseudomonas putida*. *Advances in Nanoparticles* **2013,** *2*, 287-293.

11. Tantra, R.; Jing, S. H.; Pichaimuthu, S. K.; Walker, N.; Noble, J.; Hackley, V. A., Dispersion stability of nanoparticles in ecotoxicological investigations: The need for adequate measurement tools. *Journal of Nanoparticle Research* **2011,** *13*, (9), 3765-3780.

12. El Badawy, A. M.; Luxton, T. P.; Silva, R. G.; Scheckel, K. G.; Suidan, M. T.; Tolaymat, T. M., Impact of environmental conditions (pH, ionic strength, and electrolyte type) on the surface charge and aggregation of silver nanoparticles suspensions. *Environmental Science and Technology* **2010,** *44*, (4), 1260-1266.

13. Li, X.; Lenhart, J. J.; Walker, H. W., Aggregation kinetics and dissolution of coated silver nanoparticles. *Langmuir* **2012,** *28*, (2), 1095-1104.

14. Baalousha, M.; Nur, Y.; Romer, I.; Tejamaya, M.; Lead, J. R., Effect of monovalent and divalent cations, anions and fulvic acid on aggregation of citrate-coated silver nanoparticles. *Science of the Total Environment* **2013,** *454*, 119-131.

15. Levard, C.; Hotze, E. M.; Colman, B. P.; Dale, A. L.; Truong, L.; Yang, X. Y.; Bone, A. J.; Brown, G. E.; Tanguay, R. L.; Di Giulio, R. T.; Bernhardt, E. S.; Meyer, J. N.; Wiesner, M. R.; Lowry, G. V., Sulfidation of silver nanoparticles: Natural Antidote to their toxicity. *Environmental Science and Technology* **2013a,** *47*, (23), 13440-13448.

16. Levard, C.; Mitra, S.; Yang, T.; Jew, A. D.; Badireddy, A. R.; Lowry, G. V.; Brown, G. E., Effect of Chloride on the Dissolution Rate of Silver Nanoparticles and Toxicity to *E. coli*. *Environmental Science and Technology* **2013b,** *47*, (11), 5738-5745.

17. Chen, K. L.; Elimelech, M., Aggregation and deposition kinetics of fullerene (C_{60}) nanoparticles. *Langmuir* **2006,** *22*, (26), 10994-11001.

18. Huynh, K. A.; Chen, K. L., Aggregation kinetics of citrate and polyvinylpyrrolidone coated silver nanoparticles in monovalent and divalent electrolyte solutions. *Environmental Science and Technology* **2011,** *45*, (13), 5564-5571.

19. Topuz, E.; Sigg, L.; Talinli, I., A systematic evaluation of agglomeration of Ag and TiO_2 nanoparticles under freshwater relevant conditions. *Environmental Pollution* **2014,** *193*, 37-44.

20. Topuz, E.; Traber, J.; Sigg, L.; Talinli, I., Agglomeration of Ag and TiO_2 nanoparticles in surface and wastewater: Role of calcium ions and of organic carbon fractions. *Environmental Pollution* **2015,** *204*, 313-323.

21. Hall, S.; Bradley, T.; Moore, J. T.; Kuykindall, T.; Minella, L., Acute and chronic toxicity of nano-scale TiO_2 particles to freshwater fish, cladocerans, and green algae, and

effects of organic and inorganic substrate on TiO_2 toxicity. *Nanotoxicology* **2009,** *3*, (2), 91-97.

22. Philippe, A.; Schaumann, G. E., Interactions of dissolved organic matter with artificial inorganic colloids: A review. *Environmental Science and Technology* **2014,** *48*, (16), 8946–8962.

23. Metreveli, G.; Philippe, A.; Schaumann, G. E., Disaggregation of silver nanoparticle homoaggregates in a river water matrix. *Science of the Total Environment* **2015,** *535*, (Special Issue: Engineered nanoparticles in soils and waters), 35-44.

24. Stankus, D. P.; Lohse, S. E.; Hutchison, J. E.; Nason, J. A., Interactions between natural organic matter and gold nanoparticles stabilized with different organic capping agents. *Environmental Science and Technology* **2011,** *45*, (8), 3238-3244.

25. Chen, K. L.; Elimelech, M., Influence of humic acid on the aggregation kinetics of fullerene (C_{60}) nanoparticles in monovalent and divalent electrolyte solutions. *Journal of Colloid and Interface Science* **2007,** *309*, (1), 126-134.

26. Klitzke, S.; Metreveli, G.; Peters, A.; Schaumann, G. E.; Lang, F., The fate of silver nanoparticles in soil solution - Sorption of solutes and aggregation. *Science of the Total Environment* **2015,** *535*, (Special Issue: Engineered nanoparticles in soils and waters), 54-60.

27. Furman, O.; Usenko, S.; Lau, B. L. T., Relative importance of the humic and fulvic fractions of natural organic matter in the aggregation and deposition of silver nanoparticles. *Environmental Science and Technology* **2013,** *47*, (3), 1349-1356.

28. Liu, J. Y.; Hurt, R. H., Ion release kinetics and particle persistence in aqueous nano-silver colloids. *Environmental Science and Technology* **2010,** *44*, (6), 2169-2175.

29. Newton, K. M.; Puppala, H. L.; Kitchens, C. L.; Colvin, V. L.; Klaine, S. J., Silver nanoparticle toxicity to *Daphnia magna* is a function of dissolved silver concentration. *Environmental Toxicology and Chemistry* **2013,** *32*, (10), 2356-2364.

30. Chappell, M. A.; Miller, L. F.; George, A. J.; Pettway, B. A.; Price, C. L.; Porter, B. E.; Bednar, A. J.; Seiter, J. M.; Kennedy, A. J.; Steevens, J. A., Simultaneous dispersion-dissolution behavior of concentrated silver nanoparticle suspensions in the presence of model organic solutes. *Chemosphere* **2011,** *84*, (8), 1108-1116.

31. Seitz, F.; Rosenfeldt, R. R.; Storm, K.; Metreveli, G.; Schaumann, G. E.; Schulz, R.; Bundschuh, M., Effects of silver nanoparticle properties, media pH and dissolved organic matter on toxicity to *Daphnia magna*. *Ecotoxicology and Environmental Safety* **2015,** *111*, 263-270.

32. Kretzschmar, R.; Holthoff, H.; Sticher, H., Influence of pH and humic acid on coagulation kinetics of kaolinite: A dynamic light scattering study. *Journal of Colloid and Interface Science* **1998,** *202*, (1), 95-103.

33. Baalousha, M., Aggregation and disaggregation of iron oxide nanoparticles: influence of particle concentration, pH and natural organic matter. *Science of the Total Environment* **2009,** *407*, (6), 2093-2101.

34. Liu, J. F.; Legros, S.; Ma, G. B.; Veinot, J. G. C.; von der Kammer, F.; Hofmann, T., Influence of surface functionalization and particle size on the aggregation kinetics of engineered nanoparticles. *Chemosphere* **2012,** *87*, (8), 918-924.

35. Das, P.; Xenopoulos, M. A.; Metcalfe, C. D., Toxicity of silver and titanium dioxide nanoparticle suspensions to the aquatic invertebrate, *Daphnia magna*. *Bull. Environ. Contam. Toxicol.* **2013,** *91*, (1), 76-82.

36. Lovern, S. B.; Klaper, R., *Daphnia magna* mortality when exposed to titanium dioxide and fullerene (C_{60}) nanoparticles. *Environmental Toxicology and Chemistry* **2006,** *25*, (4), 1132-1137.

37. Seitz, F.; Bundschuh, M.; Rosenfeldt, R. R.; Schulz, R., Nanoparticle toxicity in *Daphnia magna* reproduction studies: The importance of test design. *Aquatic Toxicology* **2013,** *126*, 163-168.

38. Turkevich, J.; Stevenson, P. C.; Hillier, J., A study of the nucleation and growth processes in the synthesis of colloidal gold. *Discussions of the Faraday Society* **1951,** *11*, 55-75.

39. Schultz, N.; Metreveli, G.; Franzreb, M.; Frimmel, F. H.; Syldatk, C., Zeta potential measurement as a diagnostic tool in enzyme immobilisation. *Colloids and Surfaces B-Biointerfaces* **2008,** *66*, (1), 39-44.

40. ASTM Standard E729. Standard guide for conducting acute toxicity tests on test materials with fishes, macroinvertebrates, and amphibian. **2007**.

41. Seitz, F.; Rosenfeldt, R. R.; Schneider, S.; Schulz, R.; Bundschuh, M., Size-, surface- and crystalline structure composition-related effects of titanium dioxide nanoparticles during their aquatic life cycle. *Science of the Total Environment* **2014,** *493*, 891-897.

42. Borgmann, U.; Cheam, V.; Norwood, W. P.; Lechner, J., Toxicity and bioaccumulation of thallium in *Hyalella azteca*, with comparison to other metals and prediction of environmental impact. *Environmental Pollution* **1998,** *99*, (1), 105-114.

43. Rosenfeldt, R. R.; Seitz, F.; Schulz, R.; Bundschuh, M., Heavy metal uptake and toxicity in the presence of titanium dioxide nanoparticles: A factorial approach using *Daphnia magna*. *Environmental Science and Technology* **2014,** *48*, (12), 6965-6972.

44. Loureiro, C.; Castro, B. B.; Pereira, J. L.; Goncalves, F., Performance of standard media in toxicological assessments with *Daphnia magna*: Chelators and ionic composition versus metal toxicity. *Ecotoxicology* **2011,** *20*, (1), 139-148.

45. Namvar, F.; Rahman, H. S.; Mohamad, R.; Baharara, J.; Mahdavi, M.; Amini, E.; Chartrand, M. S.; Yeap, S. K., Cytotoxic effect of magnetic iron oxide nanoparticles synthesized via seaweed aqueous extract. *Int J Nanomedicine* **2014,** *9*, 2479-88.

46. Buffle, J.; Wilkinson, K. J.; Stoll, S.; Filella, M.; Zhang, J., A Generalized description of aquatic colloidal interactions: The three-colloidal component-approch. *Environmental Science and Technology* **1998,** *32*, (19), 2887-2899.

47. Hering, J. G.; Morel, F. M. M., Humic acid complexation of calcium and copper. *Environmental Science and Technology* **1988,** *22*, (10), 1234-1237.

48. Gustafsson, J. P. Visual MINTEQ, version 3.0 (last visited: June 20, 2015). http://vminteq.lwr.kth.se/

49. Bundschuh, M.; Zubrod, J. P.; Englert, D.; Seitz, F.; Rosenfeldt, R. R.; Schulz, R., Effects of nano-TiO_2 in combination with ambient UV-irradiation on a leaf shredding amphipod. *Chemosphere* **2011,** *85*, (10), 1563-1567.

50. Derjaguin, B. V.; Landau, L., Theory of stability of highly charged lyophobic sols and adhesion of highly charged particles in solutions of electrolytes. *Acta Physiochim. (URSS)* **1941,** *14*, 633-662.

51. Verwey, E. J. W.; Overbeek, J. T. G., *Theory of Stability of Lyophobic Colloids*. Elsevier: Amsterdam, 1948.

52. Hassellov, M.; Readman, J. W.; Ranville, J. F.; Tiede, K., Nanoparticle analysis and characterization methodologies in environmental risk assessment of engineered nanoparticles. *Ecotoxicology* **2008,** *17*, (5), 344-361.

53. Finsy, R., Particle sizing by quasi-elastic light scattering. *Advances in Colloids and Interface Science* **1994,** *52*, 79-143.

54. Lin, M. Y.; Lindsay, H. M.; Weitz, D. A.; Klein, R.; Ball, R. C.; Meakin, P., Universal diffusion-limited colloid aggregation. *Journal of Physics: Condensed Matter* **1990,** *2*, (13), 3093-3113.

55. Aoki, K.; Saenger, W., Interactions of biotin with metal ions. X-ray crystal structure of the polymeric biotin-silver(I) nitrate complex: Metal bonding to thioether and ureido carbonyl groups. *Journal of Inorganic Biochemistry* **1983,** *19*, (3), 269–273.

56. Goncharova, I.; Sykora, D.; Urbanova, M., Association of biotin with silver (I) in solution: A circular dichroism study. *Tetrahedron-Asymmetry* **2010,** *21*, (15), 1916-1920.

57. Kakinen, A.; Ding, F.; Chen, P. Y.; Mortimer, M.; Kahru, A.; Ke, P. C., Interaction of firefly luciferase and silver nanoparticles and its impact on enzyme activity. *Nanotechnology* **2013,** *24*, (34), 345101.

58. Chen, R.; Choudhary, P.; Schurr, R. N.; Bhattacharya, P.; Brown, J. M.; Ke, P. C., Interaction of lipid vesicle with silver nanoparticle-serum albumin protein corona. *Appl Phys Lett* **2012,** *100*, (1).

59. Ostermeyer, A. K.; Mumuper, C. K.; Semprini, L.; Radniecki, T., Influence of bovine serum albumin and alginate on silver nanoparticle dissolution and toxicity to *Nitrosomonas europaea*. *Environmental Science and Technology* **2013,** *47*, (24), 14403-14410.

60. Li, X.; Lenhart, J. J., Aggregation and dissolution of silver nanoparticles in natural surface water. *Environmental Science and Technology* **2012,** *46*, (10), 5378-5386.

61. Munro, C. H.; Smith, W. E.; Garner, M.; Clarkson, J.; White, P. C., Characterization of the surface of a citrate-reduced colloid optimized for use as a substrate for surface-enhanced resonance Raman-scattering. *Langmuir* **1995,** *11*, (10), 3712-3720.

62. Akaighe, N.; MacCuspie, R. I.; Navarro, D. A.; Aga, D. S.; Banerjee, S.; Sohn, M.; Sharma, V. K., Humic acid-induced silver nanoparticle formation under environmentally relevant conditions. *Environmental Science and Technology* **2011,** *45*, (9), 3895-3901.

63. Adegboyega, N. F.; Sharma, V. K.; Siskova, K.; Zboril, R.; Sohn, M.; Schultz, B. J.; Banerjee, S., Interactions of aqueous Ag^{+} with fulvic acids: Mechanisms of silver nanoparticle formation and investigation of stability. *Environmental Science and Technology* **2013,** *47*, (2), 757-64.

64. Rosenfeldt, R. R.; Seitz, F.; Senn, L.; Schilde, C.; Schulz, R.; Bundschuh, M., Nanosized titanium dioxide reduces copper toxicity - The role of organic material and the crystalline phase. *Environmental Science and Technology* **2015,** *49*, (3), 1815-1822.

65. Tai, J. T.; Lai, C. S.; Ho, H. C.; Yeh, Y. S.; Wang, H. F.; Ho, R. M.; Tsai, D. H., Protein silver nanoparticle interactions to colloidal stability in acidic environments. *Langmuir* **2014,** *30*, (43), 12755-12764.

66. Field, T. B.; Coburn, J.; McCourt, J. L.; McBryde, W. A. E., Composition and stability of some metal citrate and diglycolate complexes in aqueous solution. *Analytica Chimica Acta* **1975,** *74*, (1), 101–106.

67. El Badawy, A. M.; Scheckel, K. G.; Suidan, M.; Tolaymat, T., The impact of stabilization mechanism on the aggregation kinetics of silver nanoparticles. *Science of the Total Environment* **2012,** *429*, 325-331.

68. Wang, Y.; Ni, Y. N., New insight into protein-nanomaterial interactions with UV-visible spectroscopy and chemometrics: Human serum albumin and silver nanoparticles. *Analyst* **2014,** *139*, (2), 416-424.

69. Meakin, P., Models for colloidal aggregation. *Annual Review of Physical Chemistry* **1988,** *39*, (1), 237-267.